



Effect of a Blocked Recirculation Channel on the Performance of a Not Preloaded Ball Screw with Compliant Minimal Constraints

Antonio Carlo Bertolino^(✉), Roberto Guida, Andrea De Martin, Stefano Mauro, and Massimo Sorli

Politecnico di Torino, 10129 Torino, Italy
antonio.bertolino@polito.it

Abstract. Ball screw jamming is a critical issue that can impact the performance and reliability of ball screw systems, and can lead to the loss of the entire mechanical power transmission. No dynamic analyses have been performed in the literature to study the contact conditions, dynamic behavior, and performance of the mechanism in the presence of such a fault. This paper presents the results of a simulation analysis carried out by means of a multibody dynamic model in the presence of partial jamming, obtained by blocking a sphere in one of the three recirculating channels of the considered ball screw. The model considers the full dynamics of each subcomponent and minimal compliant constraint. The effect of a blocked recirculation channel is investigated in terms of overall mechanical efficiency, the internal motion of the spheres, and their contact condition.

Keywords: ball screw · recirculation jamming · ADAMS · multibody

1 Introduction

Ball screws are widely used in various industrial and scientific applications to transmit rotary motion into linear motion. These components are widespread due to their high efficiency, precision, and durability, and they are crucial components in many machines, including CNC machines [1, 2] and aircraft actuation systems [3, 4].

However, like any mechanical component, ball screws are subject to failures and malfunctions that can impact their performance and reliability. One of the most common issues that affect ball screws is jamming, which occurs when the balls in the nut assembly get stuck and prevent the screw from rotating [5]. Ball screw jamming can lead to serious problems, such as reduced accuracy, damage to the ball screw components, and even complete system failure. The prevention and mitigation of ball screw jamming is a critical issue in the design and maintenance of ball screw systems. To achieve optimal performance and

reliability, it is essential to understand the mechanisms of ball screw jamming and develop effective strategies to prevent or mitigate this problem.

With this aim, a first cost effective approach can be to use a detailed high-fidelity model to study the effect of such problem without compromising the real component. Hitherto, several analyses in the literature focused on the study of the kinematics and dynamics of ball screws and their internal components in nominal condition, such as [6–8]. Very few researches proposed dynamic models for this mechanism: Liu et al. [9] studied the temperature effect on the drag torque generated by the preload with a computational intensive FE dynamic model in presence of lubrication. Duan et al. [10] developed a lumped parameter simplified model to study the accuracy positioning of a twin ball screw feed system. Most of dynamic models, however, do not consider the motion and dynamics of the spheres and have been used to perform vibration analyses. Only recently, fully comprehensive dynamic models have been proposed by the authors in both the Simscape [11] and MSC ADAMS [12,13] environments to investigate the ball screw mechanism under various points of view. Braccesi et al. [14] proposed an elastic-plastic model to analyse the impacts of the spheres with the recirculating deflector. A similar analysis was carried out by Hung et al. [15] who concentrated on the fracture condition of the deflector. Nevertheless, there is a lack of studies on the mechanism performances when one or multiple recirculating channels jam, especially from a dynamic point of view.

The present paper aims to fill this gap studying the performance and internal contact condition of a single-nut not preloaded ball screw in presence of a sphere stuck in one of its three recirculating circuits. The employed multibody dynamic model is firstly described together with its assumptions and limitations. Then, the results of a dynamic simulation are presented and commented.

2 Multibody Model

The MSC ADAMS software was selected as modeling environment to leverage its ability to easily describe contacts between general shaped three-dimensional bodies. Starting from a detailed CAD, the unnecessary features were removed simplifying the geometry such as nut grease refill duct, nut flange, attachments holes, chamfers, external diameter section variation, threaded shanks, screw shaft unused parts. To avoid the variation of inertial properties due to these simplifications, the total mass, the inertia tensor, the mass centre location and the principal axes of inertia orientation were imposed to the various subcomponents after their importation as parasolid format inside ADAMS, replacing the default values auto-calculated by the software from the geometry and material density. In such a way the dynamic behaviour of each body reflects the real one while a simplified geometry is only used for contact evaluation.

In fact, ADAMS internally performs a geometry discretization, approximating the surfaces of the mating bodies by means of a triangular tessellation through the RAPID algorithm: it consists in a pre-computation of a hierarchical representation of the ADAMS model using tight-fitting oriented bounding box

trees (OBBTrees), approximating thus the model with a series of polygons [16]. The contact detection is thus carried out analysing the relative intersection of the nodes of each body. Thanks to the geometry simplification, a reduced number of elements are needed to represent the helical groove surface with sufficient accuracy and, hence, less computational time is required to complete a single simulation.

The ball screw being studied has a vertical layout and is composed of a rotating screw shaft and a single non-preloaded translating nut that is subject to an external axial force as a disturbance. The motion is dictated by a prescribed speed law imposed to the screw shaft. The system presents an axisymmetric layout with three 120° outdistanced loaded circuits of spheres and three recirculation channels. The latter, schematically shown in Fig. 1, deflects the spheres from the nominal helix allowing them to be brought back by one lead overstepping the screw thread crest to the starting point of the circuit. The middle line of each sphere circuit volume was identified from the CAD and then it was used to extract the initial positions of the spheres considering homogeneous equal distancing between each ball throughout the entire path.

It is worth to be highlighted that, due to the presence of grease seals and the grease duct, the center of mass of the nut and its principal axes of inertia respectively do not perfectly lies on and align with the system symmetry axis. The same applies to the screw shaft inertial properties because of the presence of mechanical machining on its extremities.

The spheres were represented with their analytical formulation in order to save computational time. A simulation maximum time step of $2 \mu\text{s}$ has been adopted with the implicit Hilbert-Hughes-Taylor (HHT) solver, which is an appropriate stable and robust solution when dealing with stiff models and many contacts [17].

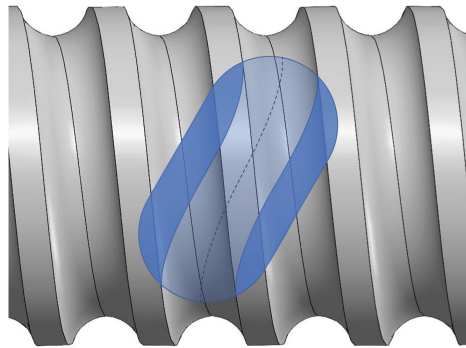


Fig. 1. Schematic representation of an internal recirculation channel.

2.1 Normal Contact

Contact is fundamentally a discontinuous event. Since numerical integrators assume a continuous solution, a contact event is a critical event since it represents a discontinuity in the solution. ADAMS works with variable step solvers and adjust the integration time step to meet the specified accuracy but also depending on its internal contact predictor, which estimates the onset of imminent contacts. When a contact is detected, the interpenetration and penetration speed are calculated to estimate a characteristic contact time, which is used to resize the integration step. Furthermore, the integrator order is modified and set to one. In fact, the predictor-corrector strategy of the ADAMS solver uses previously calculated solution values to predict its evolution; however, if a contact occurs, the future behaviour of the system does not depend anymore on many past points, hence the solver uses only the last one (order one).

All bodies are described as rigid and they should not compenetrates: the elastic deformation that usually happens in the contact area is considered within the contact constraint enforcement, consisting of a penalty regularization composed of the sum of two terms: an elastic and a damping contributions. The first depends on the penetration of the two bodies while the second is related to the energy loss during the impact due to the hysteretic behaviour of the materials and the presence of the lubricating grease. The reaction force, normal to the contact can thus be expressed as:

$$F_n = K g^e + \text{STEP}(g, 0, 0, d_{max}, c) \dot{g} \tag{1}$$

where g the bodies penetration, e the exponent of the contact mode, usually equal to 1.5 for Hertzian contacts as that of the spheres with the gothic arch groove, and K is the contact stiffness. The latter is constant throughout each simulation and has been obtained by means of the explicit non-recursive approach proposed by Antoine et al. [18] assuming a theoretical contact angle of 45° :

$$K = \frac{2^{\frac{3}{2}} E_h^*}{(\delta^*)^{\frac{3}{2}} (A_h + B_h)^{\frac{1}{2}}} \tag{2}$$

where E_h^* is the equivalent modulus of elasticity of the materials of the two contacting bodies, δ^* is the dimensionless contact deformation, dependent on the contact footprint ellipticity parameter [18], and A_h and B_h are the relative principal curvatures. The latter depend on the geometric features of the selected ball screw but mainly on the helix and contact angles and have been calculated with the simplified formulation proposed in [19].

In order to avoid unrealistic discontinuities in the contact force, the damping contribution is limited by means of the STEP function:

$$\text{STEP}(x, x_0, y_0, x_1, y_1) = \begin{cases} y_0 & x \leq x_0 \\ y_0 + (y_1 - y_0) \left(\frac{x-x_0}{x_1-x_0} \right)^2 \left(3 - 2 \frac{x-x_0}{x_1-x_0} \right) & x_0 < x < x_1 \\ y_1 & x \geq x_1 \end{cases} \tag{3}$$

which, referring to Eq. (1), modulates the damping coefficient in the range $[0 \div d_{max}]$ of the contact penetration.

2.2 Friction

After identifying the location of the contact point and outward normal, obtaining the normal and slip velocities is a straightforward process. The former is the aforementioned approaching speed \dot{g} while the latter is crucial for computing the tangential friction forces. The ADAMS software does not account for rolling friction resistance, only considering sliding and spin friction. Additionally, there is no contact stiction in ADAMS, as a small amount of sliding speed is necessary to generate friction force, preventing numerical instabilities near null relative speed values. This is achieved by establishing a coefficient of friction (COF) function against sliding speed, for which two threshold speeds must be selected to tailor the curve to the specific problem, corresponding to the adherence and sliding coefficients of friction. By choosing these two parameters it is possible to represent a COF curve typical of a lubricated contact, with the typical Stribeck COF reduction [20]. However, this function does not consider the COF increase with the relative speed. In this work a static COF $\mu_s = 0.11$ and a dynamic COF $\mu_d = 0.06$ have been considered, typical of lubricated contacts, according to [12, 21].

The spin friction torque is calculated by the software depending on the relative angular speed with respect to the common normal in the contact point. It assumes the contact area as circular with radius r_c and its value can be expressed as [22]:

$$T_{spin} = \frac{2}{3} r_c F_n \quad (4)$$

2.3 Constraints

The model has been created with the aim of reproducing as much as possible the ball screw mounting layout of the actual component installed in the experimental test bench that is being developed in our laboratories, in which the nut is mounted on a gimbal-like system to allow compensation of misalignments [23].

Therefore, minimal constraints have been imposed to the system, i.e. those necessary to guarantee the correct functionality of the system. No ideal joint are present in the model: every connection with the fixed ground has been realized by means of generalized forces in which only certain components have been activated depending on the particular constraint.

The screw shaft is supposed to only rotate, therefore the two compliant bearing supports have been represented through two elastic elements placed at its extremities, one of which capable also to bear axial loads.

For what concerns the nut, it ideally should only translate. Referring to Fig. 2 the red coordinate system, centered on its center of mass, moves with the nut, while the blue coordinate system represents its initial location and is integral

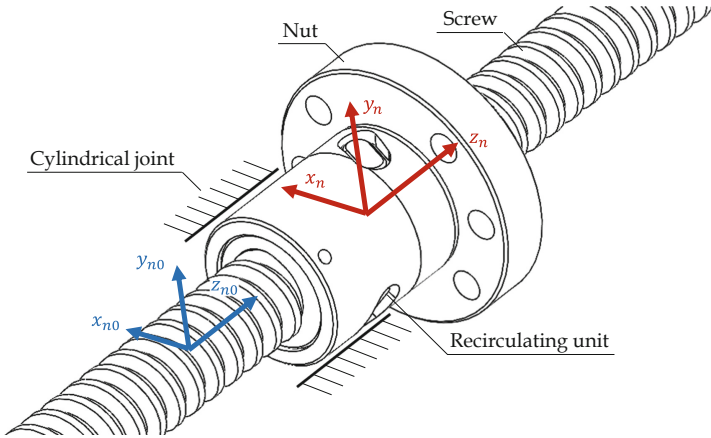


Fig. 2. Nut reference systems and constraints.

to the ground: at the beginning of a simulation, the red and blue reference systems coincide. The only constraint that has been imposed to the nut is an elastic torque which hinders the relative rotation between z_n and z_{n0} through an elastic-damping reaction torque proportional to the constraint violation. The model allows to consider joints' backlash as well, though not present in the current work. Hence, the nut is free to rotate and oscillate along the other axes and its alignment with the screw shaft is guaranteed by the presence of the contacts of the internal three circuits of spheres.

3 Simulation Results

In this section, the outcomes of a dynamic simulation using the presented model are shown, which was employed on a ball screw featuring a nominal diameter of 16 mm and 5 mm lead with three evenly spaced internal recirculation channels.

A -500 rpm speed smooth step is imposed to the screw shaft from 0.1 s to 0.2 s while an opposing external load of -1 kN is concurrently axially applied on the nut. Being right-handed, the negative speed of the screw shaft is converted into an upward velocity of the nut.

The simulation goal is to analyze the effect of a blocked sphere circuit on the performance of the mechanism. Therefore, an additional fixed constraint is added to one of the spheres within the recirculating channel of the lower sphere loop in such a way to simulate its seizure. Thus, such sphere is made integral to the nut, hindering the motion of the other balls in the same circuit thanks to the presence of the contacts between the adjacent spheres.

Figure 3 depicts the mechanical efficiency of the mechanism in nominal condition, i.e. with all the three circuits working properly, and in the case of seizure of one of them (in this work the lower one). As predictable, the mechanical efficiency reduces in the second scenario (from 0.95 to 0.79). In fact, the spheres

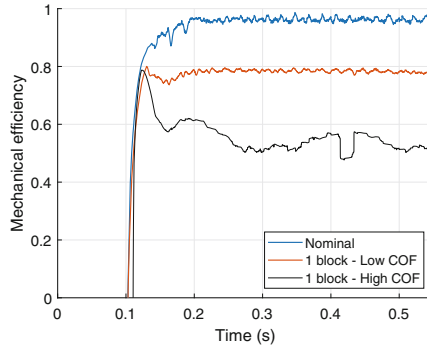


Fig. 3. Mechanical efficiency.

of the blocked circuit cannot advance in their motion through the helical path because of the sphere stuck in the recirculation channel: therefore, the basic working principal of ball screws, i.e. the rolling friction, is replaced by sliding friction. The screw groove slides on the blocked series of spheres creating more friction torque which, consequently, translates in a reduced efficiency.

However, the entity of the efficiency drop depends on the lubricating condition within the system. As observable from Fig. 3 if a static COF of $\mu_s = 0.3$ is considered, the mechanical efficiency becomes sensibly lower. Thus, depending on the COF value, the recirculation channel block can also lead to a complete jamming of the mechanism if the electrical drive cannot supply enough power to continue operating the ball screw in the new degraded conditions. If more sphere circuits jams the efficiency drops considerably further, worsening the power transmission operations.

In the healthy circuits, the spheres carry out their revolution motion around the screw shaft axis with a theoretical angular speed of approximately 24 rad/s, according to [8] for the operating conditions of the current simulation. Figure 4 shows that the revolutional speeds of the spheres in the second and third circuits correctly agree with this theoretical value. The graph represents the speed of all the 15 spheres in each circuit: when one of them enters the recirculation channel its speed decreases to come back to the nominal value after the thread crest overcome is completed. However, it can be seen that the spheres of the blocked loop start moving until they clash on the stuck one and stop moving.

While the contact forces of the spheres with the screw shaft and nut grooves varies in time, their mean value are depicted in Fig. 5. It can be seen that, being the bodies considered as infinitely rigid, the spheres in the second and third loop bears approximately the same amount of load matching the expected theoretical value of ≈ 230 N [24]. Instead, in the blocked circuit the spheres are pressed one against the other by the action of the sliding friction with the screw shaft, and tend to pile up one on the other originating a non-uniform load distribution, as shown in Fig. 5. In particular, the sphere 14 is the one which was fixed to the nut body to simulate the block and, hence, it does not present any load; the

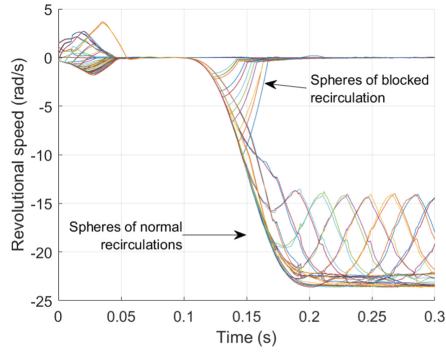


Fig. 4. Revolutional speed of the spheres of every circuit.

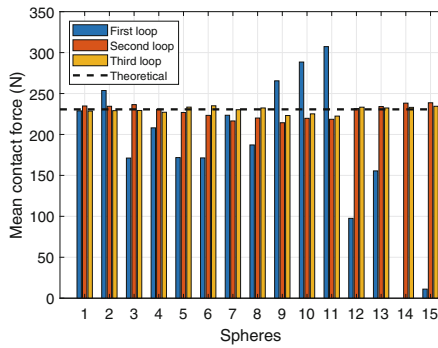


Fig. 5. Mean contact force distribution on the spheres in each sphere circuit.

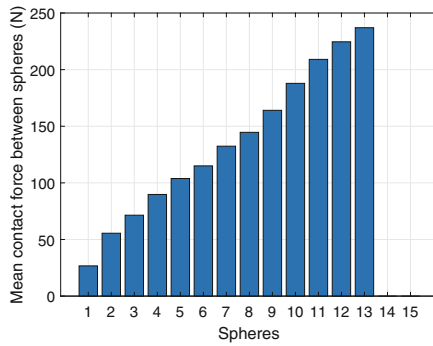


Fig. 6. Contact forces between the spheres of the blocked sphere circuit.

sphere 15 shows a very low contact force as it remains within the recirculating channel since it is not pushed out from the previous one.

The effect of the screw shaft groove sliding action can also be seen on the contact forces between adjacent spheres, shown in Fig. 6 where the horizontal axis displays the numbering of the i -th sphere contacting with the $(i + 1)$ -th. Being the 14th sphere blocked, the previous sphere (13) is pressed against it by the screw friction force and the preceding sphere, which in turn is in the same situation. Therefore, the force between the spheres varies almost linearly with the sphere position along the blocked helical path. The extent of force transmitted between consecutive spheres depends also on the mean contact force with the screw shaft of Fig. 5.

4 Conclusions

This paper analyzed the effect of a blocked recirculating channel on a not preloaded single-nut ball screw with three axisymmetric inserts. The analysis has been performed by means of a simulating analyses carried out through a multibody dynamic model developed in the MSC ADAMS environment. Non-ideal constraints have been considered for the screw shaft and the nut to represent the compliance of the supporting bearings and of the anti-rotation device. In particular, only the rotational degree of freedom about the mechanism symmetry axis has been constrained on the nut body, leaving it free to oscillate on other directions. Its correct alignment is then guaranteed by the contact forces of the spheres with the screw shaft and nut grooves and with adjacent balls. The results showed that the contact conditions on the spheres of the blocked circuit becomes more critical, especially in terms of friction. In fact, the sliding friction replaces the rolling phenomenon in the sphere/screw groove interface points, leading to a decreased mechanical efficiency. It has been also observed that the efficiency drop depends on the lubricating condition as well and can lead to a complete jamming of the entire transmission. Future developments involve the definition and development of effective strategies to prevent or mitigate this problem, one of which can be the application of prognostic algorithms. The latter can be informed and trained by detailed numerical models, such as the one presented in this work. With this goal, dedicated tests will be performed to validate the presented simulation results by means of an appositely designed test bench. Furthermore, the model will be used to study the effects of other prominent failure modes on the ball screw dynamics to lay the groundwork for the definition of future prognostics activities.



Acknowledgment.  The work was funded by the Power Electronics Innovation Center of Politecnico di Torino.

References

1. Altintas, Y., Verl, A., Brecher, C., Uriarte, L., Pritschow, G.: Machine tool feed drives. *CIRP Ann. Manuf. Technol.* **60**(2), 779–796 (2011). <https://doi.org/10.1016/j.cirp.2011.05.010>
2. Wang, D., Lu, Y., Zhang, T., Wang, K., Rinoshika, A.: Effect of stiffness of rolling joints on the dynamic characteristic of ball screw feed systems in a milling machine. *Shock Vib.* **2015** (2015). <https://doi.org/10.1155/2015/697540>
3. Bertolino, A.C., De Martin, A., Jacazio, G., Sorli, M.: A technological demonstrator for the application of PHM techniques to electro-mechanical flight control actuators. In: 2022 IEEE International Conference on Prognostics and Health Management, ICPHM 2022, pp. 70–76 (2022). <https://doi.org/10.1109/ICPHM53196.2022.9815832>, <https://ieeexplore.ieee.org/document/9815832>
4. Balaban, E., Saxena, A., Goebel, K.: Experimental data collection and modeling for nominal and fault conditions on electro-mechanical actuators. In: Annual Conference of the Prognostics and Health Management Society, pp. 1–15 (2009)
5. Hussain, Y.M., Burrow, S., Henson, L., Keogh, P.: A Review of Techniques to mitigate jamming in electromechanical actuators for safety critical applications. *Int. J. Prognost. Health Manage.* 2153–2648 (2018)
6. Yoshida, T., Tozaki, Y., Matsumoto, S.: Study on load distribution and ball motion of ball screw (2003)
7. Wei, C.C., Kao, W.H.: Analyses of contact forces and kinetic motion on heavy load ball-screw. *MATEC Web Conf.* **185**, 1–7 (2018). <https://doi.org/10.1051/mateconf/201818500014>
8. Wei, C.C., Lin, J.F.: Kinematic analysis of the ball screw mechanism considering variable contact angles and elastic deformations. *J. Mech. Des.* **125**(4), 717–733 (2003). <https://doi.org/10.1115/1.1623761>
9. Liu, D.S., Lin, P.C., Lin, J.J., Wang, C.R., Shiau, T.N.: Effect of environmental temperature on dynamic behavior of an adjustable preload double-nut ball screw. *Int. J. Adv. Manuf. Technol.* (2018). <https://doi.org/10.1007/s00170-018-2966-x>
10. Duan, M., Lu, H., Zhang, X., Zhang, Y., Li, Z., Liu, Q.: Dynamic modeling and experiment research on twin ball screw feed system considering the joint stiffness. *Symmetry* **10**(12), 686 (2018). <https://doi.org/10.3390/sym10120686>
11. Bertolino, A.C., De Martin, A., Fasiello, F., Mauro, S., Sorli, M.: A simulation study on the effect of lubricant ageing on ball screws behaviour. In: IEEE (ed.) Proceedings of the International Conference on Electrical, Computer, Communications and Mechatronics Engineering, ICECCME. IEEE, Maldives (2022). <https://doi.org/10.1109/ICECCME55909.2022.9987873>. <https://ieeexplore.ieee.org/document/9987873>
12. Bertolino, A.C., De Martin, A., Mauro, S., Sorli, M.: Multibody dynamic ADAMS model of a ball screw mechanism with recirculation channel. In: IMECE (2021). <https://doi.org/10.1115/IMECE2021-71121>. <https://asmedigitalcollection.asme.org/IMECE/proceedings-abstract/IMECE2021/85628/1132825>
13. Bertolino, A.C., De Martin, A., Sorli, M.: Performance evaluation of a ball screw mechanism through a multibody dynamic model. In: AIMETA, pp. 183–188. Palermo (2023). <https://doi.org/10.21741/9781644902431-30>, <https://www.mrforum.com/product/9781644902431-30>
14. Braccesi, C., Landi, L.: A general elastic-plastic approach to impact analysis for stress state limit evaluation in ball screw bearings return system. *Int. J. Impact Eng.* **34**(7), 1272–1285 (2007). <https://doi.org/10.1016/j.ijimpeng.2006.06.005>

15. Hung, J.P., Shih-Shyn, W.J., Chiu, J.Y.: Impact failure analysis of re-circulating mechanism in ball screw. *Eng. Fail. Anal.* **11**(4), 561–573 (2004). <https://doi.org/10.1016/j.engfailanal.2004.01.002>
16. Gottschalk, S., Lin, M.C., Manocha, D.: OBBTree: a hierarchical structure for rapid interference detection. In: *Proceedings of the ACM SIGGRAPH Conference on Computer Graphics*, pp. 171–180 (1996)
17. MSC Software: *ADAMS Solver Reference User Manual*. MSC Software (2023)
18. Antoine, J.F., Visa, C., Sauvey, C., Abba, G.: Approximate analytical model for Hertzian elliptical contact problems. *J. Tribol.* **128**(3), 660 (2006). <https://doi.org/10.1115/1.2197850>
19. Bertolino, A.C., De Martin, A., Mauro, S., Sorli, M.: Exact formulation for the curvature of gothic arch ball screw profiles and new approximated solution based on simplified groove geometry. *Machines* **11**(2), 261 (2023). <https://doi.org/10.3390/machines11020261>. <https://www.mdpi.com/2075-1702/11/2/261>
20. Zhang, L.C., Zhou, C.G.: Experimental study on the coefficient of friction of the ball screw. *J. Tribol.* **144**(3) (2022). <https://doi.org/10.1115/1.4051157>
21. Lugt, P.M.: *Grease Lubrication in Rolling Bearings*. Wiley (2013)
22. Avallone, E.A., Baumeister, T., Steidel, R.F.: *Marks' Standard Handbook for Mechanical Engineers*, 9th edn. *J. Eng. Ind.* **113**(1), 118–119 (1991). <https://doi.org/10.1115/1.2899615>. <https://asmedigitalcollection.asme.org/manufacturingscience/article/113/1/118/393095/Marks-Standard-Handbook-for-Mechanical-Engineers>
23. Bertolino, A.C., De Martin, A., Gaidano, M., Mauro, S., Sorli, M.: A fully sensorized test bench for prognostic activities on ball screws. In: *International Conference on Electrical, Computer, Communications and Mechatronics Engineering, ICECCME Oct 2021*, pp. 7–8 (2021). <https://doi.org/10.1109/ICECCME52200.2021.9591032>
24. Zhou, C.G., Feng, H.T., Chen, Z.T., Ou, Y.: Correlation between preload and no-load drag torque of ball screws. *Int. J. Mach. Tools Manuf.* **102**, 35–40 (2016). <https://doi.org/10.1016/j.ijmactools.2015.11.010>